Bio-Medical Materials and Engineering 24 (2014) 2945–2953
DOI 10.3233/BME-141114
IOS Press

Snake-based brain white matter fiber reconstruction

Meng Lu[a,*] and Jia Di[b]
[a]*College of Information Science and Engineering, Northeastern University, Shenyang 110000, China*
[b]*School of Electronic and Information Engineering, Liaoning Technical University, Shenyang 110000, China*

Abstract. Diffusion tensor imaging (DTI) is a tractography algorithm that provides the only means of mapping white matter fibers. Furthermore, because of its wealth of applications, diffusion MRI tractography is gaining importance in clinical and neuroscience research. This paper presents a novel brain white matter fiber reconstruction method based on the snake model by minimizing the energy function, which is composed of both external energy and internal energy. Internal energy represents the assembly of the interaction potential between connected segments, whereas external energy represents the differences between predicted DTI signals and measured DTI signals. Through comparing the proposed method with other tractography algorithms in the Fiber Cup test, the present method was shown to perform superiorly to the majority of the other methods. In fact, the proposed test performed the third best out of the ten available methods, which demonstrates that present method can accurately formulate the brain white matter fiber reconstruction.

Keywords: Diffusion tensor imaging, brain white matter, fiber tracking, snake model, energy minimization

1. Introduction

The unique ability of diffusion weighted MRI (DW-MRI)- based fiber tractography to map, in vivo, the architecture of white matter pathways has ignited strong interest in clinical and neuroscience research [1]. This strong interest stems from its various applications, such as an improved assessment of a range of neurological and psychiatric disorders [2] as well as characterization of anatomical connections [3]. Accordingly, the potential of tractography to help map these anatomical connections has played a significant role in motivating an ambitious project to map the human "connectome" [1].

A large number of tractography algorithms have been developed to map fibers throughout the entire brain. Of which, the most frequently used is the diffusion tensor (DT) model [4], which estimates fibers from diffusion tensor imaging (DTI). The DT model's popularity stems from the simplicity of both it as well as its imaging acquisition, which requires as few as six diffusion weighted images (DWI) and is compatible with clinical conditions. However, the largest disadvantage associated with the DT model is that only one fiber can be tracked per voxel, which means that the model performs poorly when dealing with the crossing or kissing fibers in one voxel where at least two fibers are

*Corresponding author: Meng Lu, College of Information Science and Engineering, Northeastern University, Shenyang 110000, China. Tel.: 86-18602422117; E-mail: menglu1982@gmail.com.

expected. To overcome this limitation, various other methods were proposed as alternatives, and all of which can be divided into two distinct groups: either local or global methods. Local methods construct fibers independently path-by-path; in this case, the fibers do not influence each other [5]. The reconstruction of long neuronal pathways is performed in small successive steps, either deterministic [6,7] or probabilistic[8,9] by following the local distribution of fiber directions. Conversely, global methods attempt to reconstruct the fibers simultaneously, in stark contrast to the local method process. Each fiber is assigned a probability measure that takes into account both the likelihood with the measured diffusion-weighted signal and a priori anatomical knowledge [5].

When directly compared to one another, the global methods perform much better than the local methods [1,5]. The primary reasons behind the global method's superiority are that a minor imperfection in the rule of performing local steps can accumulate and thus, significantly affect the final result, and additionally, global methods give the reconstruction a larger field of view when an ambiguous area has to be resolved. This comparison can be offered more specifically in the Fiber Cup held in London in 2009 during the Medical Image Computing and Computer Assisted Intervention (MICCAI 2009) [1].

However, in terms of time cost, local methods proceed much faster than global methods. For instance, global methods' biggest disadvantage is the high computational cost that is associated with that type of method, which consequently prohibits it from clinical practical application [10]. To solve this problem, a novel, snake model-based brain white matter fiber tractography algorithm is presented in this study. In the snake model, external energy and internal energy were used to represent the local fiber tracking procedure and the global optimum procedure, respectively, which improved the traditional global methods by using local methods to approach and accelerate the global optimization.

2. Fiber tracking method

2.1. Fiber segment simulation

Fiber segment simulation builds upon the model that was proposed by Marco Reisert and colleagues [5]. Suppose that the whole brain white matter fibers are composed of many fiber segments, and each fiber segment is a vector in the voxel, as shown in Figure 1. The vector's length is $2l$, its direction is $d=(d_1,d_2)$, $d_i \in R$, and its middle point is used to describe the vector's spatial position $p=(p_1,p_2,p_3)$, $p_i \in R$. Therefore, the positions of the vector's two endpoints are $p+ld$ and $p-ld$, respectively, and the vector can be mathematically represented by a tuple $X=(p, d)$, $p \in R^3$, $d \in R^2$. To describe the vector's endpoints, we refer to X^+ for the endpoint associated with $+n$, and X^- for the opposite endpoint associated with $-n$.

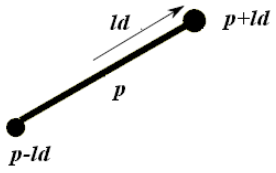

Fig. 1. Schematic diagram of the fiber segment simulation. The black bold line represents the fiber, the arrow represents the direction of the fiber that is d, p represents the fiber's middle point, $2l$ represents the fiber's length, and the two balls represent the fiber's endpoints.

The connection of two fiber segments can be transformed into the connection of two vectors, which is $C(X_1^{\alpha}, X_2^{\alpha})$, $X_i \in X$, $\alpha \in \{-,+\}$. By using α, we can know which endpoint is connected with the other fiber segment.

2.2. Global fiber tracking based on snake model

Kass Witkin and Terzopoulos first presented the snake model in 1988, and it was used to track the movement of a human's mouth [11]. The traditional snake model was used to segment image edges based on the minimization of the curve's energy, which was composed of both internal energy and external energy. The internal energy is related to the image's characters and is created by an image stress field, which can move the curve to the image edges. The external energy expresses the contour's geometric shape and restricts the contour's smoothness. Minimizing the energy is also a procedure of global optimization, which is similar to the underlying principle of the global brain white matter fiber tracking methods. Therefore, the present method further modifies and improves the traditional snake model in order to reconstruct brain white matter fibers.

In the present design, the traditional formulation of the snake model remains, as shown in Eq. (1):

$$E = \sum_{\Psi=\{X\}} (\alpha E_{\text{internal}} + \beta E_{external}) \tag{1}$$

where $\Psi = \{X\}$ represents the ensemble of fiber segments, $E_{internal}$ represents the internal energy, $E_{external}$ represents the external energy, and α and β are constants.

The definition of external energy is based upon work conducted by Marco Reisert and colleagues[5], which refers to the fiber tracking cost in the whole brain, as shown in Eq. (2):

$$E_{external} = \sum_{\Omega=\{C\}} U(X_1^{\alpha_1}, X_2^{\alpha_2}) \tag{2}$$

where $\Omega=\{C\}$ represents the ensemble of fiber connections, U represents the interaction potential between two connected segments X_1 and X_2, $X_1=(p_1,d_1)$ $X_2=(p_2,d_2)$, and $\alpha_i \epsilon \{+,-\}$. Therefore, U is defined as:

$$U(X_1^{\alpha_1}, X_2^{\alpha_2}) = \frac{1}{l^2}(\|p_1 + \alpha_1 l d_1 - \overline{p}\|^2 + \|p_2 + \alpha_2 l d_2 - \overline{p}\|^2) \tag{3}$$

where $\overline{p}$ represents the middle point of the line connecting p_1 and p_2.

Internal energy refers to the squared difference between the measured signal and the predicted signal:

$$E_{\text{internal}} = \sum_{R^3 \times R^2} | F_{measured}(p,d) - F_{predicted}(p,d) |^2 \tag{4}$$

where $p \epsilon R^3$ represents the fiber's position, $d \epsilon R^2$ represents the fiber's direction, and p and d create a scalar, which is $\mathbb{R}\, R^3 \times R^2 \mapsto R$.

The predicted signal is calculated based on the diffusion tensor two-compartment model. In this model, it is an assumption that all fibers pass through a voxel in the same direction. Assuming there is no diffusion-diffusion exchange, a simple two-compartment partial volume model is generated. The first compartment can model diffusion in and around the axons, with diffusion only in the fiber direction. However, the second models the diffusion of free water in the voxel as isotropic [12].

Therefore, the predicted signal is:

$$\mu_i = S_0((1-f)\exp(-b_i d) + f\exp(-b_i d r_i^T RAR^T r_i)) \tag{5}$$

where d represents the diffusivity, b_i represents the b-value, r_i represents the gradient direction associated with the i^{th} acquisition, f and RAR^T represent the fraction of signal contributed by, and anisotropic diffusion tensor along, (θ, ϕ) represents the fiber's direction. Additionally, A is fixed as:

$$A = \begin{pmatrix} 1 & 0 & 0 \\ 0 & 0 & 0 \\ 0 & 0 & 0 \end{pmatrix} \tag{6}$$

In addition, R rotates A to (θ, ϕ).

Based on Bayes's theorem, each of these parameters (S_0, d, f, θ, and ϕ) is subject to a prior distribution:

$$\begin{aligned} &p(\theta,\phi) \propto \sin(\theta) \\ &p(S_0) \sim U(0,\infty) \\ &p(f) \sim U(0,1) \\ &p(d) \sim \Gamma(a_d, b_d) \end{aligned} \tag{7}$$

The Markov Chain Monte Carlo (MCMC) estimation is performed for the diffusion tensor two-compartment model. Parameters are initialized with a least-square's diffusion tensor fit. The Markov Chains are then jumped 500 times without sampling as a "burn-in," followed by 2000 times and then sampling every second jump to give 1000 samples. Samples are drawn from the Metropolis Hastings samples for all parameters [12].

2.3. Minimization

The minimization of the traditional snake model is performed by making the expression's derivative as zero to iteratively calculate the result. However, as the implementation of traditional minimization in global fiber tracking is too expensive to compute, the present method respectively minimizes both the internal energy and external energy.

The external energy is composed of the squared distances from the segments' endpoints to the midpoint of the line connecting p_1 and p_2, which is shown in Figure 2. Therefore, external energy is minimized by the following rules: the coordinates x_1, x_2 should be consistent with the internal direction

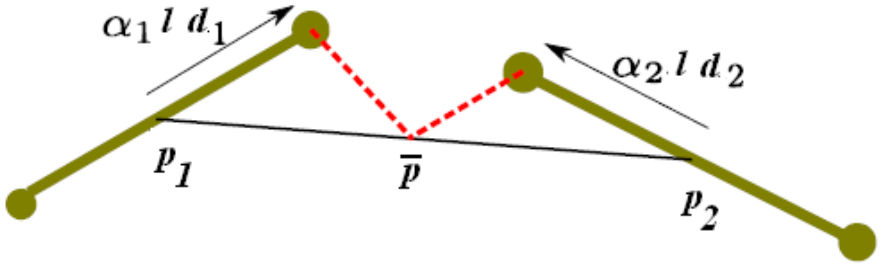

Fig. 2. External energy between two fiber segments. The dotted line is the target that should be minimized.

d_1 and d_2, which means that the connecting line between x_1 and x_2 should not differ too much. In Figure 2, the dotted line is the target that should be minimized.

Internal energy is defined as Eq. (4). This equation refers to the squared difference between the measured signal and the predicted signal, which are primarily related to the position and direction of fiber tracking in the voxel. Moreover, the fiber tracking's position in each voxel is nearly identical, so direction becomes the predominant influence for the internal energy minimization. Then, Eq. (4) can be transformed into:

$$E_{\text{int}\,ernal} = \sum_{R^2} | F_{measured}(d) - F_{predicted}(d) |^2 \tag{8}$$

Where $F_{measured}(p)$ is obtained from the diffusion tensor imaging data, and $F_{predicted}(p)$ is obtained by the diffusion tensor two-compartment model. Based on Eq. (7), the direction of the predicted signal (θ, ϕ) is subject to the prior distribution $\sin(\theta)$. Therefore, in each voxel, the direction that is closest to the measured direction can be chosen as the signal's predicted direction. However, one more impact has to be considered: that is, the probability density of the chosen direction neighborhood cannot be too small, as shown in Eq. (9). Otherwise, the chosen direction value rarely occurs, and the accumulative effect may produce an unrealistic fiber tracking result.

$$\int_{\theta-\Delta}^{\theta+\Delta} \sin(\theta) d\theta \geq \varepsilon \tag{9}$$

where Δ represents the neighborhood of the chosen direction, and ε represents the lower limit of the probability density, which in the present method is $\varepsilon=0.1$.

3. Experiments and results

The experimental design in this study consisted of two parts: the phantom fiber tracking test and real brain white matter fiber tracking test. Firstly, the present method was used to reconstruct fiber tracking based on a phantom. Since the ground truth of the phantom's fiber tracking results was already known, the present method's accuracy could be clearly obtained via comparison. Then, the present method was used to reconstruct fiber tracking based on real brain white matter data in order to demonstrate a practical clinic result.

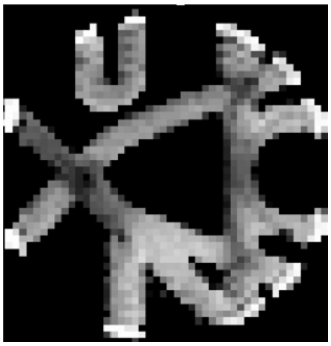

Fig. 3. ADC image of the phantom dataset

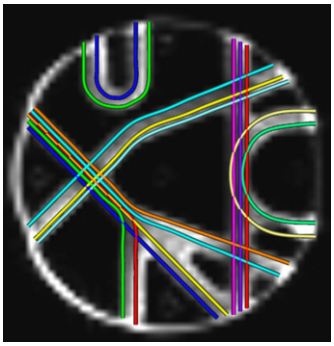

Fig. 4. Ground truth fiber tracking for the phantomDataset; there are seven most prominent bundles.

3.1. Phantom fiber tracking test

The phantom was from the Fiber Cup held in London in 2009 during the Medical Image Computing and Computer Assisted Intervention (MICCAI 2009) [1] and is publicly available on the following website: http://www.lnao.fr/spip.php?rubrique79. This phantom's associated advantages are: (1) this phantom was elaborately manufactured (the whole procedure can be referred to from [1] and [13]); (2) this phantom contained various extreme conditions of fiber tracking: fiber crossing, fiber kissing, as well as bundles of different curvatures; (3) many famous fiber tracking methods [14–23] have already conducted testing on this phantom and have been given a score based on an evaluation system, so the present method can be quantitatively compared with the previous tracking methods.

The parameters for the phantom acquisition were as follows: spatial resolution was 3 mm, field of view FOV=19.2 cm, matrix 64×64, slice thickness TH=3 mm, read bandwidth RBW=1775 Hz/pixel, partial Fourier factor 6/8, parallel reduction factor GRAPPA=2, repetition time TR=5 s, 2 repetitions, b-value=1500 s/mm^2, diffusion sensitization corresponding to the echo times TE=94 ms, and SNR=2.6. An ADC image of the phantom is given in Figure 3, and the ground truth of the phantom is shown in Figure 4.

The phantom's fiber tracking reconstruction results are shown in Figure 5, and there are seven most prominent bundles. Figure 5(A) and Figure 5(B) show the reconstruction result of the high curvature fibers; Figure 5(C) and Figure 5(D) show the reconstruction result of the crossing fibers; and finally, Figure 5(E), Figure 5(F), and Figure 5(G) show the reconstruction result of the kissing fibers. From the given results, it is clear that the present method can resolve all of these complicated fiber configurations in the phantom test.

The evaluation system of phantom analysis also gives a score for the reconstruction results, which allows for quantitative comparisons between different methods. This evaluation system relies upon the point-based Root Mean Square Error (RMSE) between the construction results and the ground truth [1]. The other ten methods and their associated scores are the following (listed in decreasing score order): Global tractography [5] 116 score, FOD-SH with constrained spherical deconvolution and streamline tractography [16] 87 score, Combined 2-DT model estimation and streamline tractography [19] 31 score, ODF-SH with positivity and regularity constraints and streamline tractography [23] 19 score, PAS-MRI and streamline tractography [20] 16 score, Adaptive 1 or 2-DT model and streamline tractography [15] 5 score, Single-DT and streamline tractography [21] 5 score, FOD-SH with

streamline tractography [22] 5 score, Single-DT with tensor deflection [18] 4 score, and Single-DT with streamline tractography and RK4 integration [4] 0 score. The present method obtained a score of 78, placing it third in the previous list. Such a score means that, while the present method is superior to the majority of the other methods, there is still room for improvement. Notably, the global tractography method took two of the top-three places; however, streamline tractography (the method that represents the local tractography method) placed in the bottom five spots.

3.2. Real brain white matter fiber tracking test

The real brain DWI data was taken from a 17-year-old boy with a left-side motor seizure. The image acquisition parameters are as follows: 32 directions; six-channel sensitivity encoding; sensitivity encoding factor of two; b-value=600 sec/mm^2; FOV, 220×220 mm; and section thickness=2.3 mm.

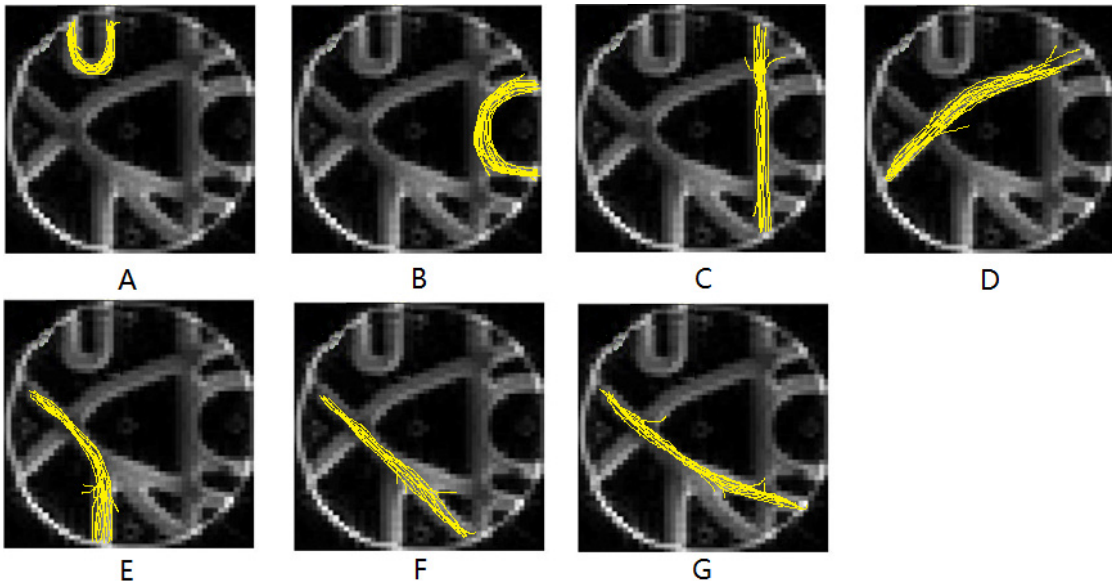

Fig. 5. Phantom fiber tracking results; the seven most prominent bundles are shown.

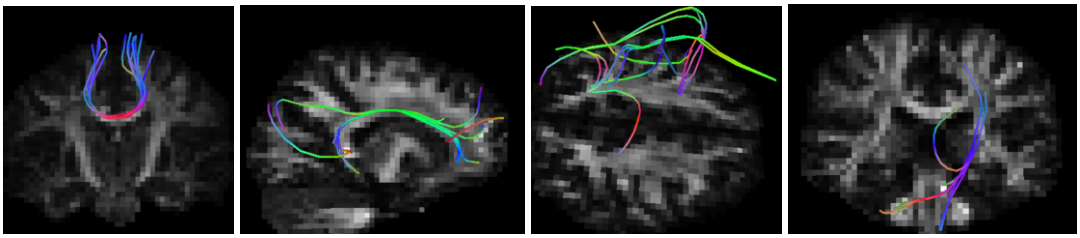

(a) CCtoM1 (b) CG (c) IFO (d) CST

Fig. 6. Diagram of several well-known fiber bundles: (a) callosal fibers coming from the left motor cortex (CCtoM1), (b) the cingulum (CG), (c) the inferior fronto-occipital fasciculus (IFO), and (d) corticospinal tracts to the left motor cortex (CST).

Our method's computation time was compared with Jbabdi's global tractography based on Bayesian framework [24]. Both methods ran on the same computer workstation to reconstruct the whole brain white matter fiber tracking. Our method's computation time is about 50 minutes, whereas the other needs several hours because of the huge computational cost of MCMC calculation.

As shown in Figure 6, several regions of interest (ROI) were selected to extract well-known fiber bundles: which are, callosal fibers coming from the left motor cortex (CCtoM1), the cingulum (CG), the inferior fronto-occipital fasciculus (IFO), and corticospinal tracts to the left motor cortex (CST). All these extracted bundles coincide with the brain's anatomy and physiology. Therefore, the brain white matter fiber reconstruction result can be a source of both essential information and guidance for clinical and neuroscience research.

4. Conclusion

This paper presented a novel brain white matter fiber reconstruction method based upon the snake model, which is a means of globally tracking all the white matter fibers by minimizing the energy function. After conducting comparisons with other methods in the Fiber Cup test, the present method was determined to have a performance superior to the majority of other available methods. In fact, the proposed method performed the third best out of ten other methods, meaning the offered brain white matter fiber reconstruction method can accurately track the fibers as well as reasonably deal with the crossing, kissing, and high curvature fibers.

Acknowledgement

This paper was supported by the National Natural Science Foundation of China (No.61101057) and the Fundamental Research Funds for the Central Universities (No. N130404027).

References

[1] F. Pierre, D. Maxime, G. Alvina et al., Quantitative evaluation of 10 tractography algorithms on a realistic diffusion MR phantom, NeuroImage **56** (2011), 220–234.
[2] O. Ciccarelli, M. Catani, H. Johansen-Berg et al. Diffusion-based tractography in neurological disorders: concepts, applications, and future developments, Lancet Neurol. **7** (2008), 715–727.
[3] H. Johansen-Berg and M. Rushworth, Using diffusion imaging to study human connectional anatomy, Lancet Neurol. **32** (2009), 75–94.
[4] P. Basser, J. Mattiello and D. Lebihan, Estimation of the effective self-diffusion tensor from the NMR spin echo, Journal of Magnetic Resonance **103** (1994), 247–254.
[5] R. Macro, M. Irina, A. Constantin et al., Global fiber reconstruction becomes practical, NeuroImage **54** (2011), 956–962.
[6] S. Mori, B.J. Crain and V.P. Chacko, Three-dimensional tracking of axonal projections in the brain by magnetic resonance imaging, Ann Neurol. **45** (1999), 265–269.
[7] P.J. Basser, S. Pajevic and C. Pierpaoli, In vivo fiber tractography using DT–MRI data, Magnetic Resonance Medicine **44** (2000), 625–632.
[8] P. Hagmann, J.P. Thiran, L. Jonasson et al., Dti mapping of human brain connectivity: statistical fibre tracking and virtual dissection, NeuroImage **19** (2003), 545–554.
[9] G.J.M. Parker, H.A. Haroon and C.A.M. Wheeler-Kingshott, A framework for a streamline-based probabilistic index of connectivity (pico) using a structural interpretation of mri diusion measurements, Journal of Magnetic Resonance Imaging **18** (2003), 242–254.

[10] B.W. Kreher, I. Mader and V.G. Kiselev, Gibbs tracking: a novel approach for the reconstruction of neuronal pathways, Magnetic Resonance Medicine **60** (2008), 953–963.
[11] M. Kass and A. Witkin, Snakes: active contour models, International J of Computer Vision **1** (1988), 321–331.
[12] T.E.J. Behrens, M.W. Woolrich, M. Jenkinson et al., Characterization and propagation of uncertainty in diffusion-weighted MR imaging, Magnetic Resonance in Medicine **50** (2003), 1077–1088.
[13] C. Ponpon, B. Rieul, L. Kezele et al., New diffusion phantoms dedicated to the study and validation of HARDI models, Magnetic Resonance in Medicine **60** (2008), 1276–1283.
[14] A. Ramirez-Manzanares, M. Rivera and B. Vemuri, Diffusion basis functions decomposition for estimating white matter intravoxel fiber geometry, IEEE Transactions on Medical Imaging **26** (2007), 1091–1102.
[15] A. Ramirez-Manzanares, M. Rivera and J.C. Gee, Depicting axon fibers on a diffusion phantom by means of hybrid DBF-DT data, MICCAI Workshop on Diffusion Modelling and the Fiber Cup, London, United Kingdom, 2009.
[16] B. Jeurissen, A. Leeman, J. D. Tournier et al. Fiber tracking on the 'fiber cup phantom' using constrained spherical deconvolution, MICCAI workshop on Diffusion Modelling and the Fiber Cup, London, United Kingdom, 2011.
[17] F. Tensaouti, J.A. Lotterie and I. Berry, Fiber tracking on the phantom dataset by using Sisyphe software, MICCAI workshop on Diffusion Modelling and the Fiber Cup, London, United Kingdom, 2009.
[18] M. Lazar, D. Weinstein and J. Tsuruda, White matter tractography using diffusion tensor deflection, Human Brain Mapping **18** (2003), 306–321.
[19] J.G. Malcolm, M.E. Shenton and Y. Rathi, Filtered multi–tensor tractography, IEEE Transactions on Medical Imaging **29** (2010), 1664–1675.
[20] S. Mori, B. Crain and V. Chacko, Three-dimensional tracking of axonal projections in the brain by magnetic resonance imaging, Ann Neurol **45** (1999), 481–492.
[21] P. Fillard, J. Gilmore and W. Lin, Quantitative analysis of white matter fiber properties along geodesic paths, Proc. of MICCAI'03, Part I **2879** (2003), 16–23.
[22] M. Descoteaux, R. Deriche and T. Knosche, Deterministic and probabilistic tractography based on complex fibre orientation distributions, IEEE Transactions on Medical Imaging **28** (2009), 269–286.
[23] A. Goh, Deterministic tractography using orientation distribution functions estimated with probability density constraints and spatial regularity, MICCAI workshop on Diffusion Modelling and the Fiber Cup, London, United Kingdom, 2009.
[24] S. Jbabdi, M.W. Woolrich, J.L.R. Andersson and T.E.J. Behrens, A Bayesian framework for global tractography, NeuroImage **37** (2007), 116–129.